Supporting Information

Nucleic acid-selective light-up fluorescent biosensors for ratiometric two-photon imaging the viscosity of live cells and tissues

Dandan Li, Xiaohe Tian, Aidong Wang, Lijuan Guan, Jun Zheng, Fei Li, Shengli Li, Hongping Zhou, Jieying Wu, Yupeng Tian*

Contents

Materials and apparatus....1
Synthetic procedures of dyes DSF and DBF....4
Crystal structure of DSF....6
Absorption and emission spectra of DSF and DBF....7
The water solubility of DSF and DBF....8
The effect of PH for DSF and DBF....9
One-Photon Excited Fluorescence (OPEF) response to solvent viscosity....9
Cytotoxicity and photostability of DSF and DBF....10
DNA binding studies of DSF....11
Live cell uptake of DBF....13
Interaction with amino acids and biomolecules....14
Possible influencing factors on targeting and localization properties....15
Characterization....18

Materials and apparatus

All chemicals and solvents were dried and purified by the standard methods. Elemental analysis was performed on a Perkin–Elmer 240C elemental analyzer. IR spectra were recorded with a Nicolet FTIR Nexus 870 instrument in the range 4000–400 cm^{-1} by using KBr pellets. ^{1}H and ^{13}C NMR spectra were recorded on a 400 and 100 MHz NMR instrument

using $(CD_3)_2SO$ as solvent. Chemical shifts were reported in parts per million (ppm) relative to internal TMS (0 ppm) and coupling constants in Hz. Splitting patterns were described as singlet (s), doublet (d), triplet (t), quartet (q), or multiplet (m). The linear absorption spectra were measured on a SPECORD S600 spectrophotometer. The single-photon emission fluorescence (SPEF) spectra measurements were performed using a Hitachi F-7000 fluorescence spectrophotometer. The two-photon emission fluorescence (TPEF) spectra were measured at femtosecond laser pulse and Ti: sapphire system (680–1080 nm, 80 MHz, 140 fs) as the light source.

HepG2 cells were luminescently imaged on a Zeiss LSM 710 META upright confocal laser scanning microscope. Image data acquisition and processing was performed using Zeiss LSM Image Browser, Zeiss LSM Image Expert and Image J.

X-ray crystallography: The X-ray diffraction measurements were performed on a Bruker SMART CCD area detector using graphite monochromated Mo-K_α radiation (λ = 0.71069 Å) at 298(2)K. Intensity data were collected in the variable ω-scan mode. The structures were solved by direct methods and difference Fourier transformations. The non-hydrogen atoms were refined anisotropically and hydrogen atoms were introduced geometrically. Calculations were performed with SHELXTL-97 program package

Viscometry: The viscosities of the solvents were determined using capillary Ubbelohde dilution type viscometers, which were submerged in a temperature bath with ±0.1°C accuracy. The viscosity calibration solutions were prepared by dilution of glycerol or sucrose in water.Average kinematic viscosity was taken as themeanof three offlowingtime measurements, then converted to intrinsic viscosity by correction for appropriate density. Higher viscosities of the aqueous solution of glycerol were taken from published tables.[1]

DNase and RNase treatment: HepG2 cells were fixed in paraformaldehyde at 4°C for 10 min. The cell membrane was permeablized with 1% TritonX-100 in PBS for 1min at room temperature and then washed with PBS twice. For RNase (DNase) digest test, two sets of prefixed HepG2 cells were stained with 10 μM DSF and DBF in PBS (pH = 7.4) for 30 min. After rinsing with PBS twice, a total 1 mL PBS (as control experiment) was added into a set of cells and 25 mg/mL DNase-Free RNase (RNase-Free DNase) was added into the other set of cells, and then two sets of cells were incubated at 37 °C in 5% CO_2 for 2 h. After rinsing with PBS twice, both two sets of

cells were imaged with wide-field fluorescence microscopy. In addition, the RNase (DNase) digest test of cells stained with 1 mM RNA-Select (Hoechst 33342) was also carried out for comparison.

Cytotoxicity test: The study of the effect of DSF and DBF on viability of cells was carried out using the methylthiazolyldiphenyl-tetrazolium bromide (MTT) assay. DSF or DBF stock solutions were diluted by fresh mediumin to desired concentration (5, 10, 15, 20, 25 μM). HepG2 cells were cultured in a 96-well plate for 24h before experiments. The cell medium was then exchanged by different concentrations of DSF or DBF medium solutions. They were then incubated at 37 °C in 5% CO_2 for 24 h before cell viability was measured by the MTT assay. The cell medium solutions were exchanged by 100 μL of fresh medium, followed by the additionof 20 μL (5 mg/mL) MTT solution to each well. The cell plates were then incubated at 37 °C in 5% CO_2 for 4 h. Absorbance was measured at 570 nm. The absorbance measured for an untreated cell population under the same experimental conditions was used as the reference point to establish 100% cell viability. Duplicated experiments have been tested.

Cell culture and staining: For HepG2 cells (liver hepatocellular carcinoma, ATCC No. HB-8065), the medium used was Dulbecco's modified Eagle's medium (DMEM) supplemented with 10% fetal calf serum (FCS, GIBCO), penicillin and streptomycin, L-glutamine and fungizone. For live cell confocal laser scanning microscopy experiment, HepG2 cells were seeded in 24-well glass bottom plate (In Vitro Scientific, P24-1.5H-N) at density of 10,000, and incubated for 72-96 hours at 37 °C in 95% air 5% CO_2 in order to allow the cells to reach ~90% confluence, the medium changed every two days. DSF and DBF were prepared as 1mM PBS solution, and dilute in culture medium at 10 μM for 30 min at 37 °C in 95% air 5% CO_2 and then imaged with confocal microscopy. RNA-Select was dissolved in DMSO at a concentration of 1 mM and Hoechst 33342 was prepared as 1 mM aqueous solution.

For colocalization experiments, DSF or DBF (10 μM) was incubated with HepG2 cells in DMEM for 30 min, and then the medium were replaced with fresh medium in the presence of SYTO RNA-Select (1 μM) or Hoechst 33342 (1 μM) for 30 min. The 24-well plate were washed by PBS twice and imaged.

Fresh tissue staining and culture: Specific pathogen Free（SPF) KM (Kunming) mouse(male, two month, 18-22g）was terminally anaesthetised and transcardially perfused with phosphate

buffered saline (PBS) 0.1M pH 7.4. The liver was extracted and the tissue was then snap frozen in liquid nitrogen cooled isopentane. Fresh frozen organs from PBS-perfused animals were sectioned at 200 μm in the sagittal plane using a cryostat (Leica 1950). The fresh tissue incubated with 10 μM DSF or DBF solution for 30 minutes at 37 °C in 95% air 5% CO_2, then washed with PBS buffer 3 times. Tissue was mounted cover-slipped using an aqueous Prolong Diamond Antifade medium without DAPI (Life Technology P36970), and imaged directly using a Zeiss LSM 710 upright confocal system. Microscopy: HepG2 Cells and liver tissues were luminescently imaged on a Zeiss LSM 710 META upright confocal laser-scanning microscope. For live-cell imaging, an incubation chamber was applied, connected to ZEISS temperature control unit 37°C and CO_2 controller (1-2 hours before the experiment was allowed for stabilization of the temperature and CO_2 concentration). The acquisition of co-localisation data by means of Pearson's correlation coefficient was done via an ImageJ plug-in 'Colocalization Finder' (Dye A = red, Dye B = Green). Rr (-1< Rr <1) refers to the Pearson correlation coefficient, where: Rr = 1 = perfect colocalization; Rr = 0 = random localization; Rr = -1 = perfect exclusion.

Note: All procedures involving animals were approved by and conformed to the guidelines of the Anhui University Animal Care Committee. We have taken great efforts to reduce the number of animal used in these studies and also taken effort to reduce animal suffering from pain and discomfort.

Synthetic procedures of dyes DSF and DBF

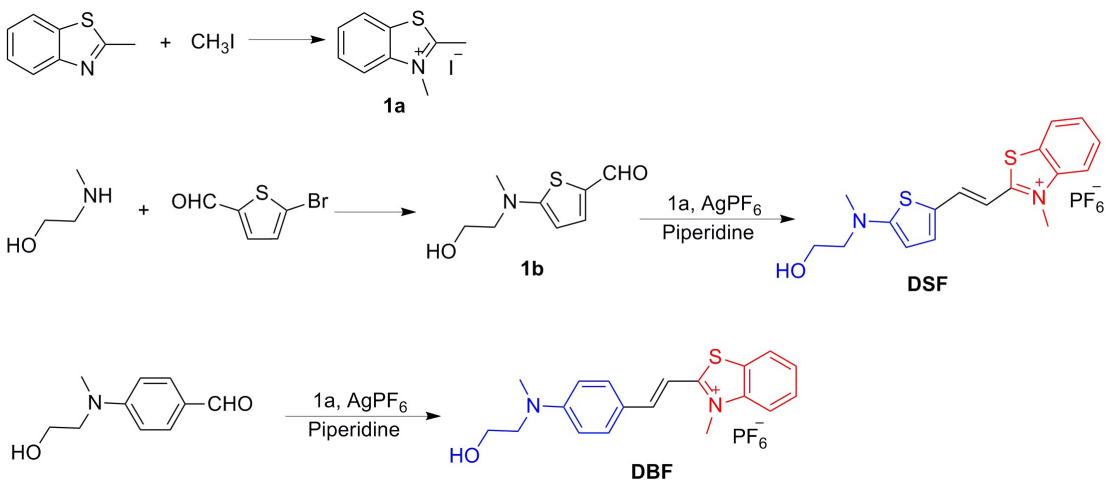

Figure S1. The Synthetic procedures of dyes DSF and DBF

Methyl iodide (0.85g, 6 mmol) was added under nitrogen to 2-methyl benzothiazole (0.90g, 6 mmol) with stirring at 60-70 °C for 3 h. The mixture was then cooled, the precipitate filtered off, and washed with ether to give 2,3-dimethylbenzothiazolium iodide, 2,3-dimethylbenzothiazolium iodide salt 1a was obtained as white solid as crude product (1.6 g, yield 91%). ^{1}H NMR: (400Hz, d_6-DMSO), δ (ppm): 8.43 (d, J = 8.1 Hz, 1H), 8.29 (d, J = 8.5 Hz, 1H), 7.90 (t, J = 7.9 Hz, 1H), 7.81 (t, J = 7.7 Hz, 1H), 4.20 (s, 3H), 3.16 (s, 3H).

A 0.86 g (4.5 mmol) amount of 5-Bromothiophene-2-carbaldehyde, 1.13 g (15 mmol) of 2-(Methylamino)ethanol, and 0.1 g of toluene-4-sulfonic acid were mixed and stirred at a bath temperature of 100 °C for 20 h. The mixture was cooled, and 25 mL of water was added. The organic layer and dichloromethane extracts were combined, washed with water, and dried over Mg_2SO_4. Evaporation of the solvent, purification by column chromatography. 5-((2-hydroxyethyl)(methyl)amino)thiophene-2-carbaldehyde 1b was obtained as yellow solid (0.29 g, yield 35%). Mp: 83 °C. ^{1}H NMR: (400Hz, d_6-DMSO), δ (ppm): 9.40 (s, 1H), 7.65 (d, J = 4.4 Hz, 1H), 6.12 (d, J = 4.4 Hz, 1H), 4.87 (t, J = 5.4 Hz, 1H), 3.62 (q, J = 5.5 Hz, 2H), 3.47 (t, J = 5.6 Hz, 2H), 3.09 (s, 3H). ^{13}C NMR (100 MHz, d_6-DMSO) δ 179.2, 167.2, 141.5, 124.6, 103.2, 57.8, 56.9, 40.7.

Using a 100 mL one-necked flask fitted with a stirrer and a condenser, 0.29 g (1.0 mmol) of 1a, 0.18 g (1.0 mmol) of 1b, and 30 mL of absolute ethanol were mixed. Five drops of piperidine were added to the mixture. Then the solution was heated to reflux for 4 h. After cooling, 0.25 g (1.0 mmol) of $AgPF_6$ was added into the solution. The solution again was heated to reflux for 30 min. A purple solid formed after cooling. The solution was filtered, and the solid was washed twice with ethanol. Pueple solid product **DSF** was collected (0.40 g, yield 85%). Mp: 186 °C. ^{1}H NMR (400 MHz, d_6-DMSO) δ 8.08 (t, *J* = 12.1 Hz, 1H), 7.84 (d, *J* = 8.3 Hz, 1H), 7.64 (t, *J* = 7.9 Hz, 1H), 7.50 (t, *J* = 7.7 Hz, 1H), 6.56 (s, 1H), 5.01 (t, *J* = 5.2 Hz, 1H), 3.97 (s, 1H), 3.80 – 3.59 (m, 2H), 3.28 (s, 1H). ^{13}C NMR (100 MHz, d_6-DMSO) δ 179.7, 171.5, 167.9, 161.2, 142.6, 141.9, 128.9, 126.2, 125.4, 123.7, 114.34, 109.9, 98.5, 58.5, 42.1, 34.6. FT-IR (KBr, cm^{-1}): 3235(s), 2920 (w), 1642 (w), 1590 (s), 1520 (m), 1474 (w), 1435 (w), 1372 (m), 1329 (m), 1162 (s), 1039 (m), 943 (w), 881 (w), 811 (w), 612 (w), 548 (w). M^+ (MS/ESI), 331.25.

0.29 g (1.0 mmol) of 1a, 0.18 g (1.0 mmol) of 4 – N - methyl – N - (hydroxyethyl) amino) benzaldealde, and 30 mL of absolute ethanol were mixed. Five drops of piperidine were added to

the mixture. Then the solution was heated to reflux for 4 h. After cooling, 0.25 g (1.0 mmol) of $AgPF_6$ was added into the solution. The solution again was heated to reflux for 30 min. A red solid formed after cooling. The solution was filtered, and the solid was washed twice with ethanol. Red solid product **DBF** was collected (0.40 g, yield 85%). Mp: 192 °C. ^{1}H NMR (400 MHz, d_6-DMSO) δ 8.29 (d, *J* = 8.0 Hz, 1H), 8.07 (dd, *J* = 15.7, 11.9 Hz, 2H), 7.89 (d, *J* = 8.9 Hz, 2H), 7.79 (t, *J* = 7.8 Hz, 1H), 7.68 (t, *J* = 7.7 Hz, 1H), 7.61 (d, *J* = 15.3 Hz, 1H), 6.88 (d, *J* = 9.0 Hz, 2H), 4.82 (s, 1H), 4.23 (s, 3H), 3.68 – 3.55 (m, 4H), 3.12 (s, 3H). ^{13}C NMR (100 MHz, d_6-DMSO) δ 171.5, 153.5, 150.3, 142.2, 133.4, 128.9, 127.7, 126.9, 123.8, 121.4, 116.4, 112.5, 106.9, 58.5, 54.1, 35.9. FT-IR (KBr, cm^{-1}): 3237(s), 2969 (w), 1642 (w), 1583 (s), 1524 (s), 1469 (w), 1435 (w), 1407 (m), 1326 (m), 1173 (s), 1151 (s), 1038 (m), 834 (w), 769 (w), 727 (w), 612 (w), 549 (w). M^+ (MS/ESI), 325,25.

Crystal structure of DSF

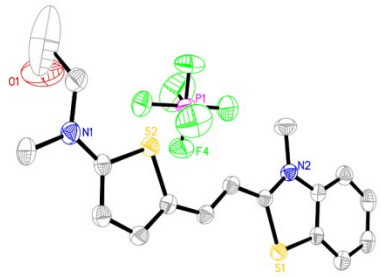

Figure S2. The crystal structure of DSF.

Table S1 Crystal data collections and structure refinements of **DSF**

	DSF	
Empirical formula	$C_{17}H_{19}F_6N_2OPS_2$	
Formula weight	476.43	
Crystal system	Triclinic	
Space group	P$\bar{1}$	
Unit cell dimensions	a= 7.645(5)Å	α= 95.390(5)°
	b= 11.246(5)Å	β= 105.282(5)°
	c= 12.326(5)Å	γ= 93.459(5)°
Volume	1013.7(9) Å^3	

Absorption coefficient	0.407 mm^{-1}
Reflections collected / unique	7154 / 3522 [R(int) = 0.0383]
Max. and min. transmission	0.9231 and 0.8877
Data / restraints / parameters	3522 / 0 / 265
Goodness-of-fit on F^2	1.042
R_1, wR_2 (all data)	R_1 = 0.0943, wR_2 = 0.2238
Largest diff. peak and hole	0.758 and -0.773 e. $Å^{-3}$

Absorption and emission spectra of DSF and DBF

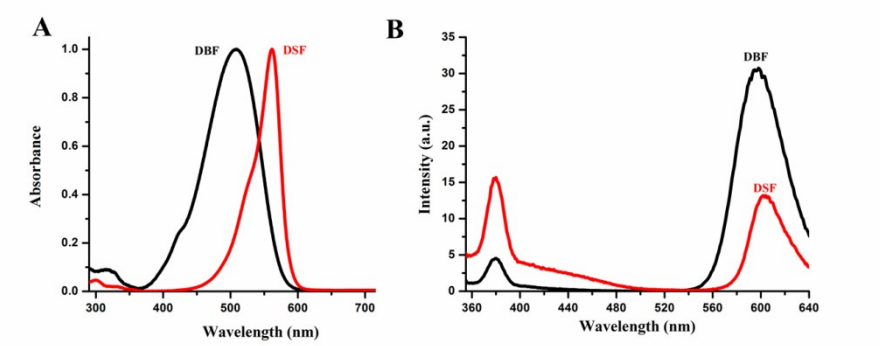

Figure S3. The normalized absorption (Left) and emission (Right) spectra of dyes DSF and DBF in aqueous solution.

As seen in Figure S3, DSF and DBF have two absorption peaks (λ_{abs} 300, 560 and 320, 505 nm in aqueous solution, respectively) and two emission peaks (λ_{em} 380, 605 and 380, 597 nm in aqueous solution, respectively).

The water solubility of DSF and DBF

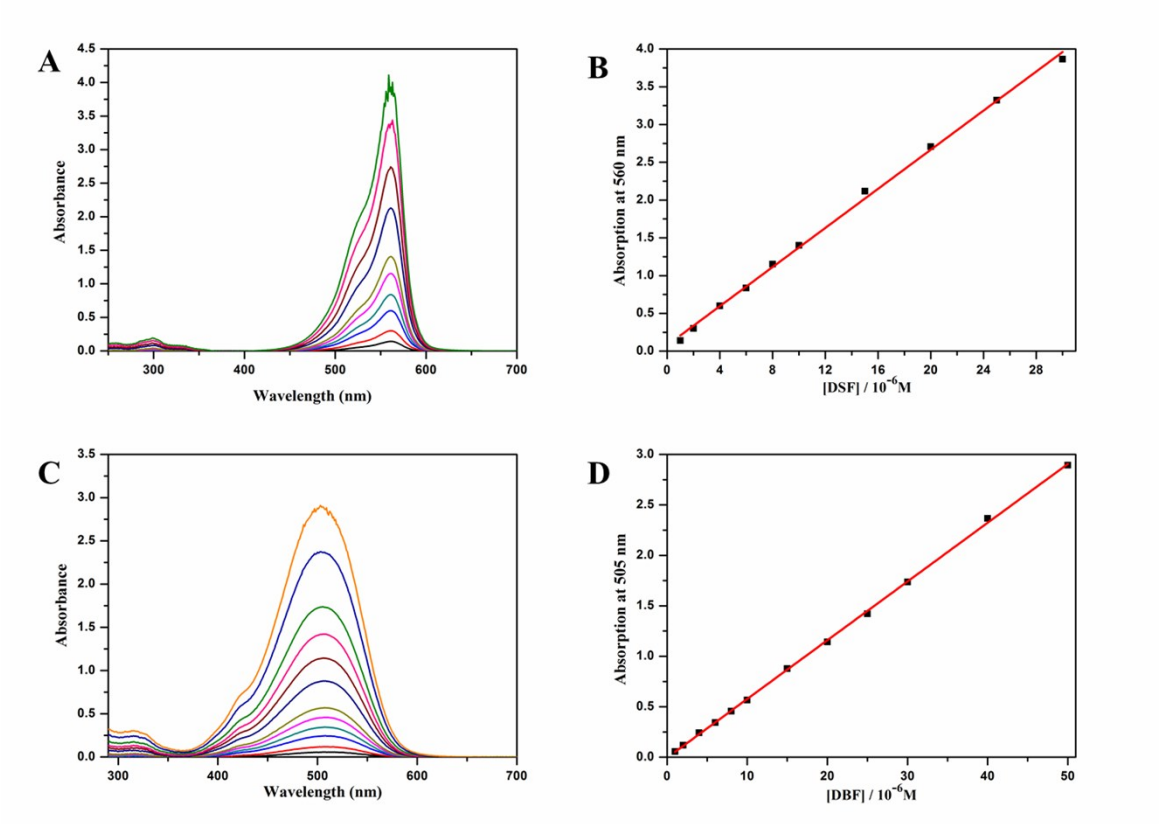

Figure S4. Absorption spectra (A and C) and plot of intensity against the concentration (B and D) of dyes DSF and DBF in pure PBS buffer (PH = 7.4), respectively.

As shown in Fig. S4, probes DSF and DBF are soluble in pure PBS buffer (PH = 7.4), and at least 30 μM solution of DSF (50 μM solution of DBF) could be obtained, which is sufficient to stain the living samples.

The effect of PH for DSF and DBF

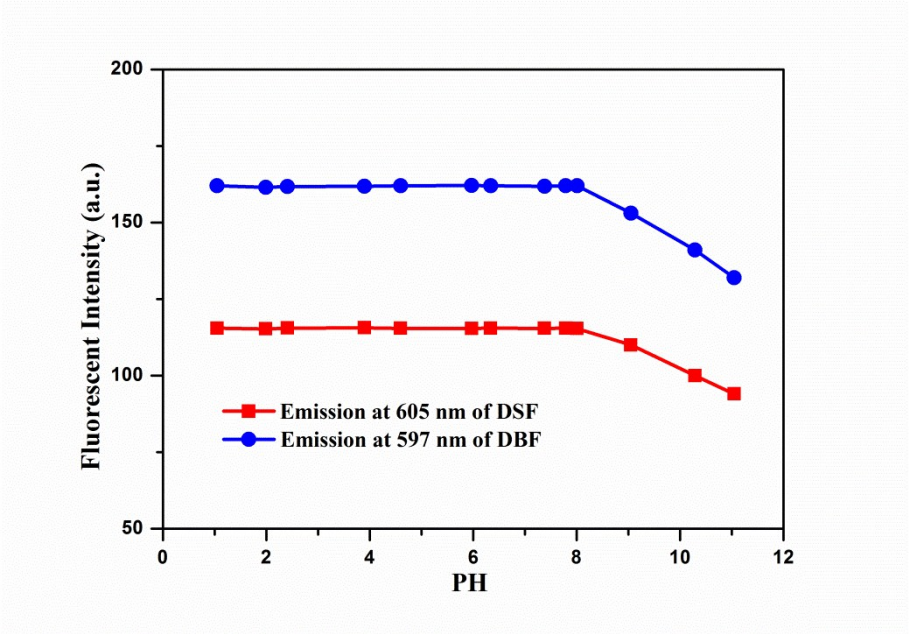

Figure S5. The fluorescent intensities for DSF and DBF at varied PH values.

The effect of PH for DSF and DBF were investigated by emission spectra changes. As shown in Fig. S5, the probes DSF and DBF are stable in a PH region of 1-8.

One-Photon Excited Fluorescence (OPEF) response to solvent viscosity

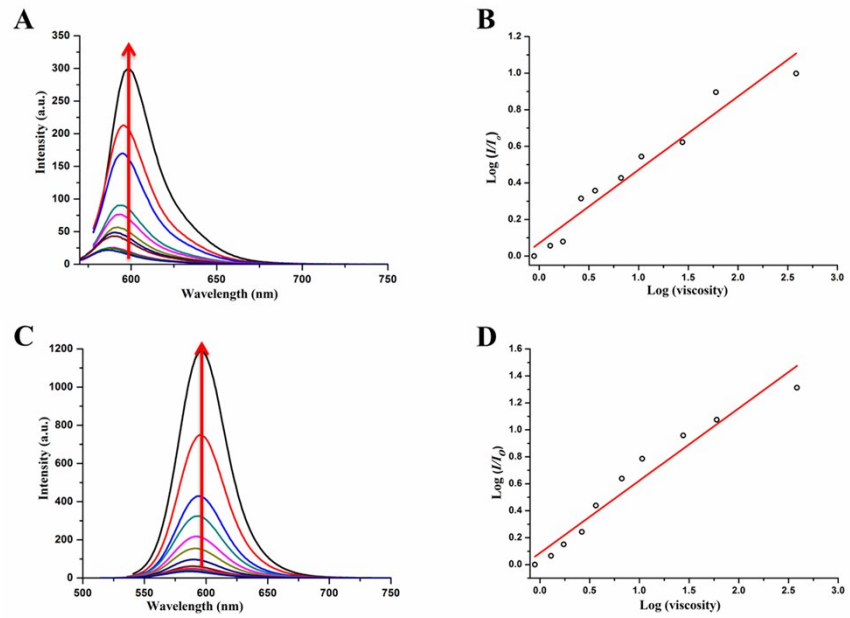

Figure S6. A) The red-fluorescence-emission spectra of DSF as a function of solvent viscosity (excited at 560 nm); B) the linear response between log (I/I_0) and log (viscosity) in the water/glycerol solvent (excited at 560 nm) of DSF; C) The red-fluorescence-emission spectra of DBF as a function of solvent viscosity (excited at 505 nm); D) the linear response between log (I/I_0) and log (viscosity) in the water/glycerol solvent (excited at 505 nm) of DBF.

As shown in Figure S6A and B, we investigated the red emission spectra of DSF in mixtures of water and glycerol. The emission of rotor DSF was greatly enhanced when excited at 560 nm. The emission intensity at 605 nm in glycerol was 15-fold that seen in water, and the logarithm of the fluorescence ratio thereof (I/I_0) at 605 nm showed a good linear relationship with that of the viscosity of the solution. The R^2 of 0.94 and the slope x of 0.40 indicate that DSF could be applied with the fluorescence-enhancement method that senses the viscosity change quantitatively. Additionally, the red emission spectra of DBF in mixtures of water and glycerol were investigated as well (Figure S6C and D). The emission intensity at 597 nm in glycerol was 40-fold that seen in water when excited at 505 nm, and the logarithm of the fluorescence ratio thereof (I/I_0) at 597 nm showed a good linear relationship with that of the viscosity of the solution (R^2 = 0.95, x = 0.54). This demonstrated that DBF could be employed to ratiometrically detect the solution viscosity.

Cytotoxicity and photostability of DSF and DBF

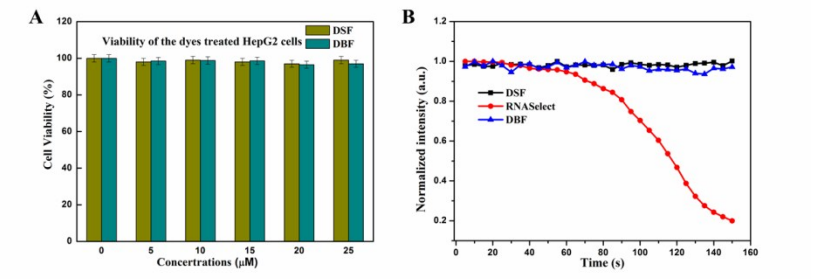

Figure S7. Cytotoxicity and photostability of DSF and DBF: A) Cytotoxicity of DSF and DBF; B) photostability of DSF (10 μM), DBF (10 μM) and RNASelect (1 μM).

The two important factors for evaluating applicability of new fluorescent probes in live cell imaging are cytotoxicity and photostability. Therefore, the cytotoxicity of DSF and DBF toward HepG2 cell lines was studied by MTT assay (Fig. S7A). The results show that DSF and DBF

exhibited good cell tolerability at imaging concentration after 24 h of incubation. In addition, the photostability of DSF, DBF and RNASelect in cell imaging were also examined. The dyes DSF and DBF exhibited better photostability than RNASelect. The fluorescence signals of DSF and DBF showed nosignificant decrease under continuous irradiation for 150 s. By contrast, the fluorescence signals of RNASelect decreased by 80% (Fig. S7B), indicating that DSF and DBF are promising sensors for cell imaging.

DNA binding studies of DSF

UV-vis absorption spectroscopy is one of the most helpful methods to study the interactions between biosensors and DNA, and the biosensors binding to DNA commonly results in hypochromism (decrease in absorbance) and bathochromism (red shift).[2] The UV-vis absorption spectra of the DSF in the absence and the presence of ct-DNA are shown in Fig. S8. As increasing the ct-DNA concentration, the absorption of DSF exhibited hypochromism and slight bathochromism. The evident spectral changes indicate that there are strong interactions between DSF and ct-DNA, and DSF can bind to ct-DNA non-electrostatically.

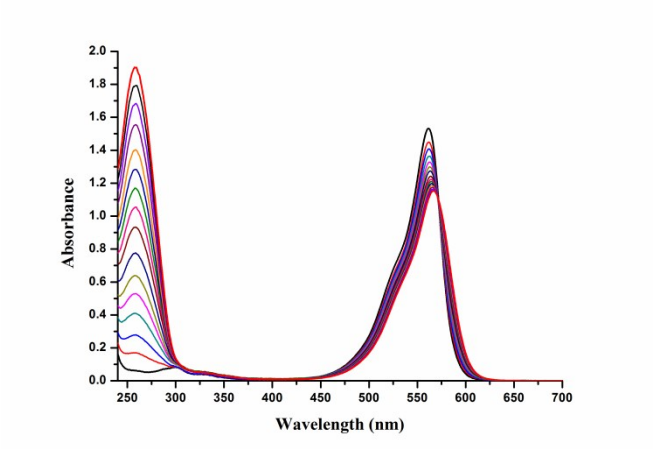

Figure S8. Changes in UV-visible absorption spectrum of DSF (Tris buffer (5mM tris(hydroxymethyl)aminomethane, 25 mM NaCl, pH = 7.4) with addition of ct-DNA.

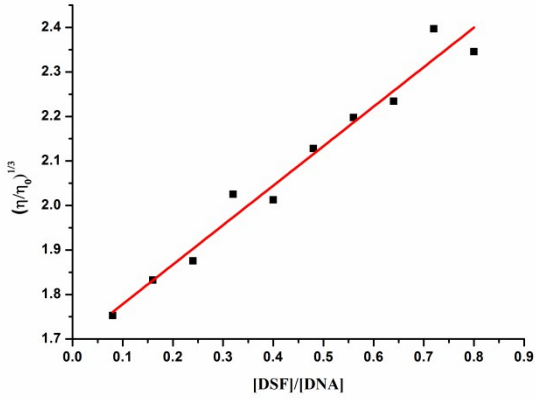

Figure S9. Plot of relative viscosity of DNA upon addition of DSF (Tris buffer).

It is known that intercalating moieties unwind DNA, thus increasing relative viscosities of aqueous DNA solutions, while groove-binding and electrostatically molecules demonstrate no such effect.[3] Therefore, to further explore the interaction of DSF and DNA, the relative viscosity of calf thymus DNA upon the addition of DSF was measured. Fig. S9 indicates that the addition of DSF to DNA results in an increase of the specific viscosity. These results reveal that there are strong interactions between DSF and ct-DNA due to the stacking interactions between the aromatic ring and the base pairs of DNA.

Table 2. The Properties of DSF/DBF, classical dyes and of the Reference Compounds.

Compound	Target	Binding mode	Water-soluble	Molecular weight (g/mol)	Cell Viability	Photostability	2PA activity
DSF	DNA	Intercalation	Good	476.06	>95% (25 μM)	High	Optimized
DBF	RNA	Unknown	Good	470.10	>95% (25 μM)	High	Optimized
DAPI	DNA	Groove binding	Poor	277.32	Poor	Low	Not optimized
EB	DNA	Intercalation	Poor	394.31	Poor	Low	None
SYTO 9	RNA	Not discussed	Poor	Unknown	Poor	Low	None

TP-2Bzim (Reference I)	DNA	Groove binding	Not discussed	547.65	Cell permeant	High	Optimized
CP (Reference II)	RNA	Not discussed	Not discussed	460.15	>95% (10 μM)	High	None

Reference I: B. Dumat, G. Bordeau, E. Faurel-Paul, F. Mahuteau-Betzer, N. Saettel, G. Metge, C. Fiorini-Debuisschert, F. Charra and M. P. Teulade-Fichou, *J. Am. Chem. Soc*, 2013, **135**, 12697-12706.

Reference II: B. Zhou, W. Liu, H. Zhang, J. Wu, S. Liu, H. Xu and P. Wang, *Biosens. Bioelectron.*, 2015, **68**, 189-196.

Live cell uptake of DBF

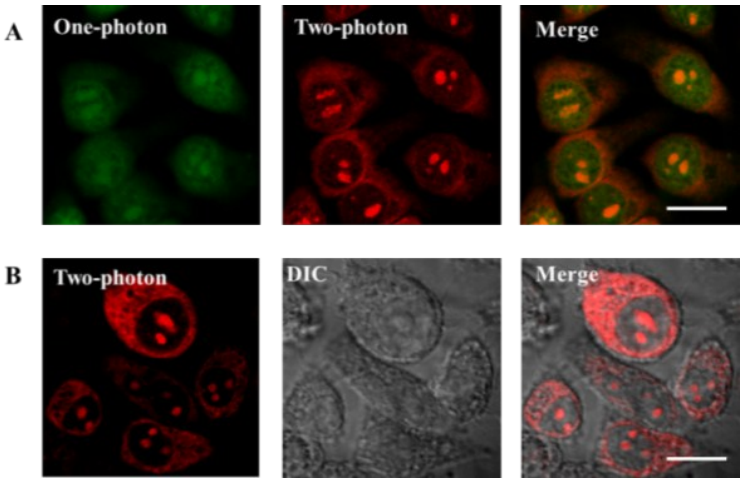

Figure S10. A) One and two-photon fluorescent images of living cells by DBF. One and two-photon excitation were at 488 and 800 nm, respectively: OPM image of DBF (570-610 nm), TPM image of DBF (580-620 nm); B) Two-photon fluorescent and DIC images of living cells by DBF. Scale bar: 20 μm.

Interaction with amino acids and biomolecules

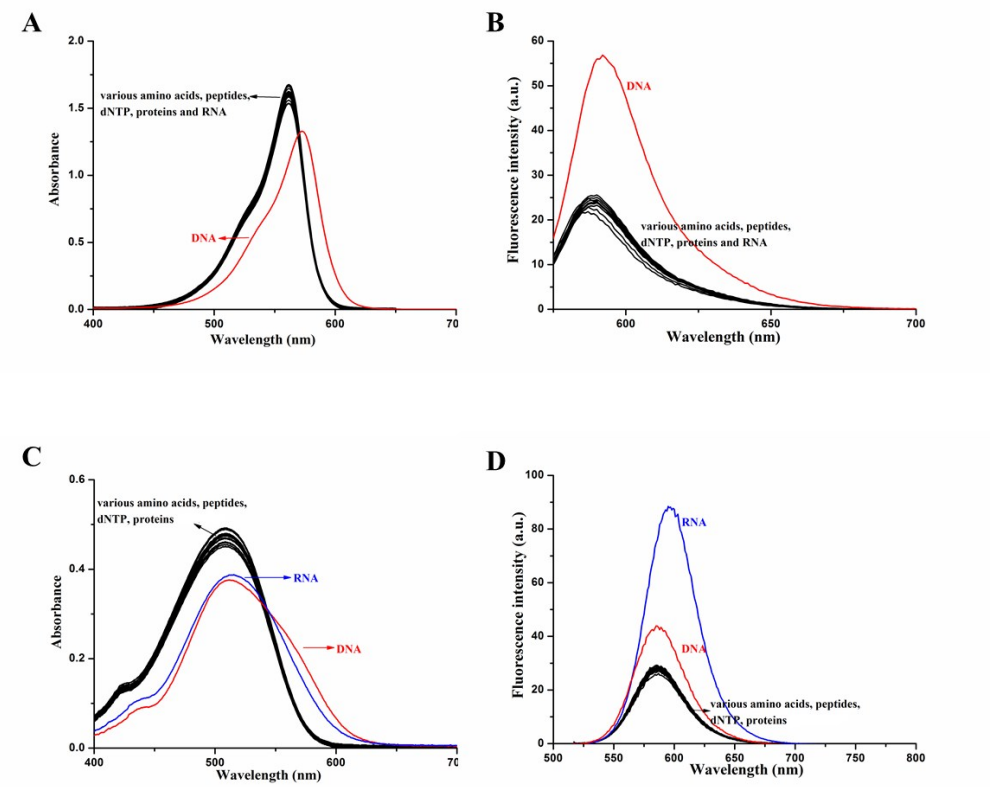

Figure S11. Absorption and fluorescence spectra changes of 10 μM DSF (A, B) and 10 μM DBF (C, D) with 100 μM various natural amino acids [such as L-alanine (Ala), L-arginine (Arg), L-asparagine (Asp), L-glutamine (Gln), L-glycine (Gly), L-isoleucine (Ile), L-leucine (Leu), L-lysine (Lys), L-phenylalanine (Phe), L-proline (Pro), L-serine (Ser), L-threonine (Thr), L-tryptophan (Try), L-tyrosine (Tyr), L-valine (Val), L-glutamic acid (Glu), L-cysteine (Cys), L-methionine (Met), L-histidine (His)], BSA, 2'-deoxyadenosine-5'-triphosphate (dATP), 2'-deoxycytidine-5'-triphosphate (dCTP), 2'-deoxyaguanosine-5'-triphosphate (dGTP), 2'-deoxythymidine-5'-triphosphate (dTTP), RNA, and DNA in PBS (PH = 7.4).

Table S3. The fluorescence quantum yields of DSF and DBF in presence of NA.

Probe / Solution	PBS	DNA (Tris-buffer)	RNA (Tris-buffer)
DSF	1.56%	8.68%	2.92%
DBF	2.19%	7.86%	13.44%

Possible influencing factors on targeting and localization properties.

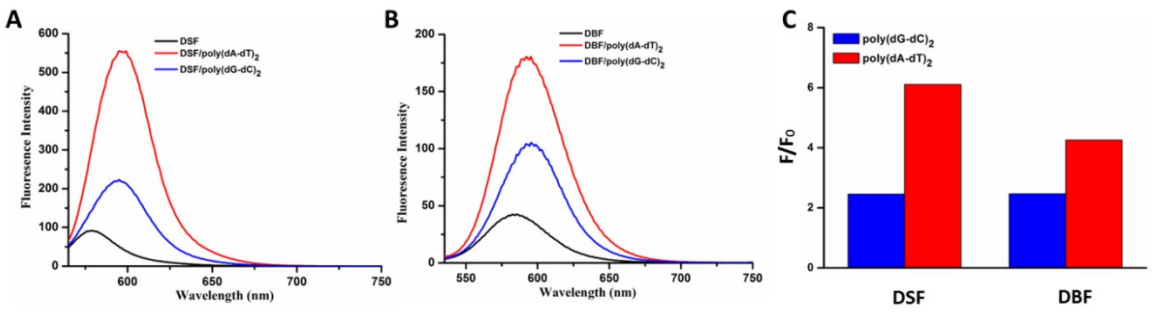

Figure **S12**. A) Fluorescence spectra change of DSF in polynucleotides poly(dA.dT)$_2$ and poly(dG.dC)$_2$ [DSF] = 1 μM in PBS, pH 7.4; B) Fluorescence spectra of DBF in polynucleotides poly(dA.dT)$_2$ and poly(dG.dC)$_2$ [DBF] = 1 μM in PBS, pH 7.4; C) Fluorescence enhancement factor (bar diagram).

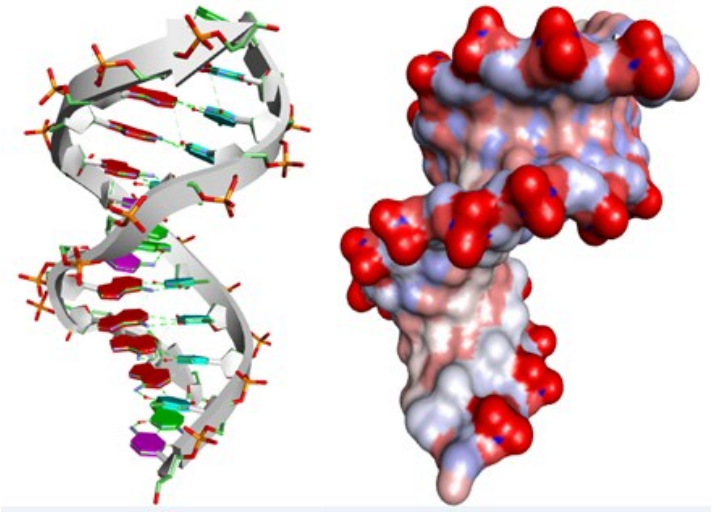

Figure **S13**. The structure of corresponding DNA fragment (base sequences CTTTTGCAAAAG/CTTTTGCAAAAG).

Table S4. The CDOCKER energy of docking probes.

Molecule	CDOCKER energy (Kcal/mol)	Average CDOCKER energy (Kcal/mol)
DSF	-35.4842	-34.4496
DSF	-35.4631	
DSF	-35.0587	
DSF	-34.9055	
DSF	-34.8556	
DSF	-34.3896	
DSF	-33.9858	

DSF	-33.908	
DSF	-33.2454	
DSF	-33.2002	
DBF	-35.2601	-33.1579
DBF	-34.2657	
DBF	-34.044	
DBF	-33.9729	
DBF	-33.8119	
DBF	-32.6748	
DBF	-32.6263	
DBF	-32.0212	
DBF	-31.4778	
DBF	-31.425	

CDOCKER_ENERGY Optimized: CDOCKER interaction score (negative of the energy) after optimizing the hydrogen position at the ligand and on the receptor in the vicinity of the ligand.

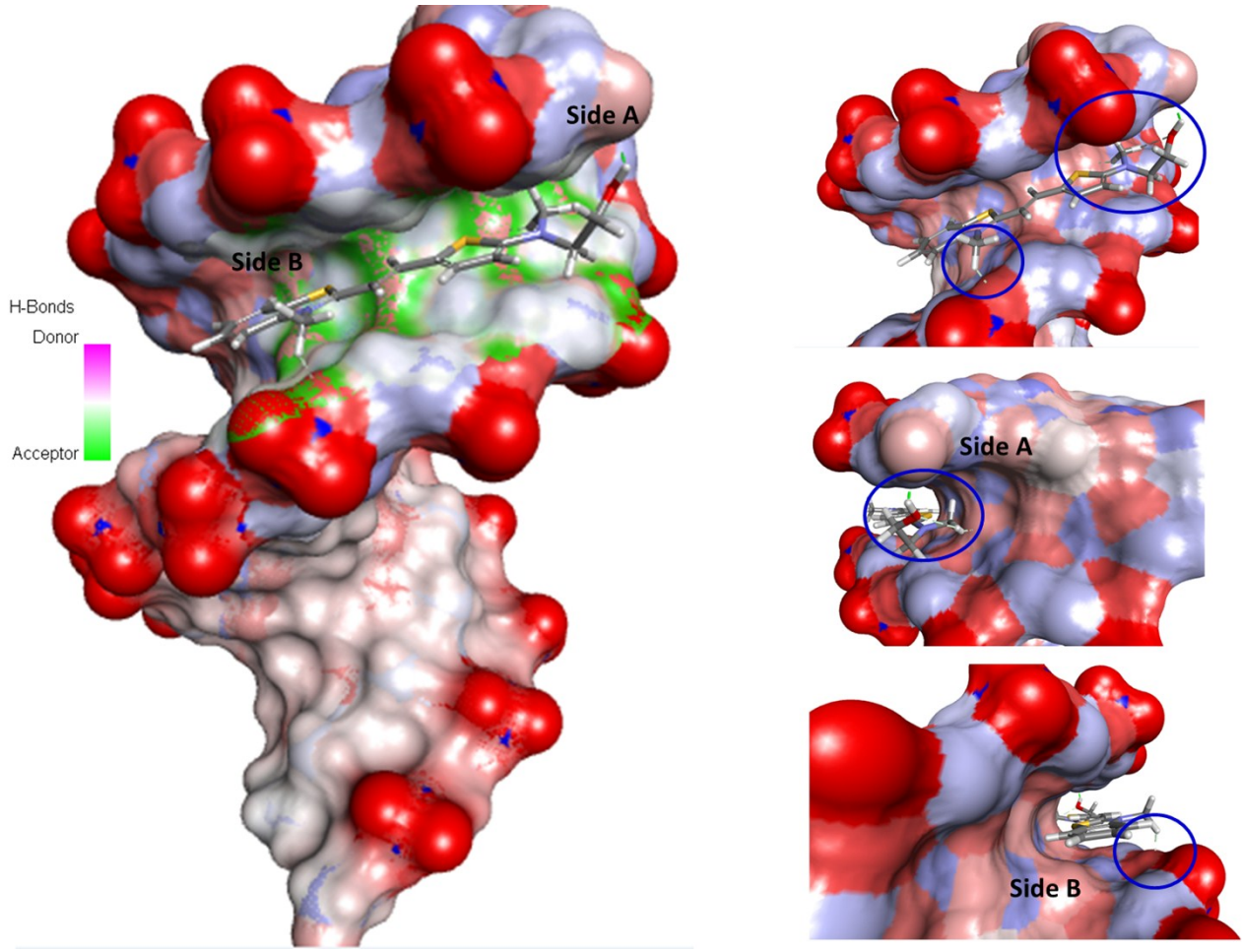

Figure S14. The side view of the interaction of DSF with DNA fragment.

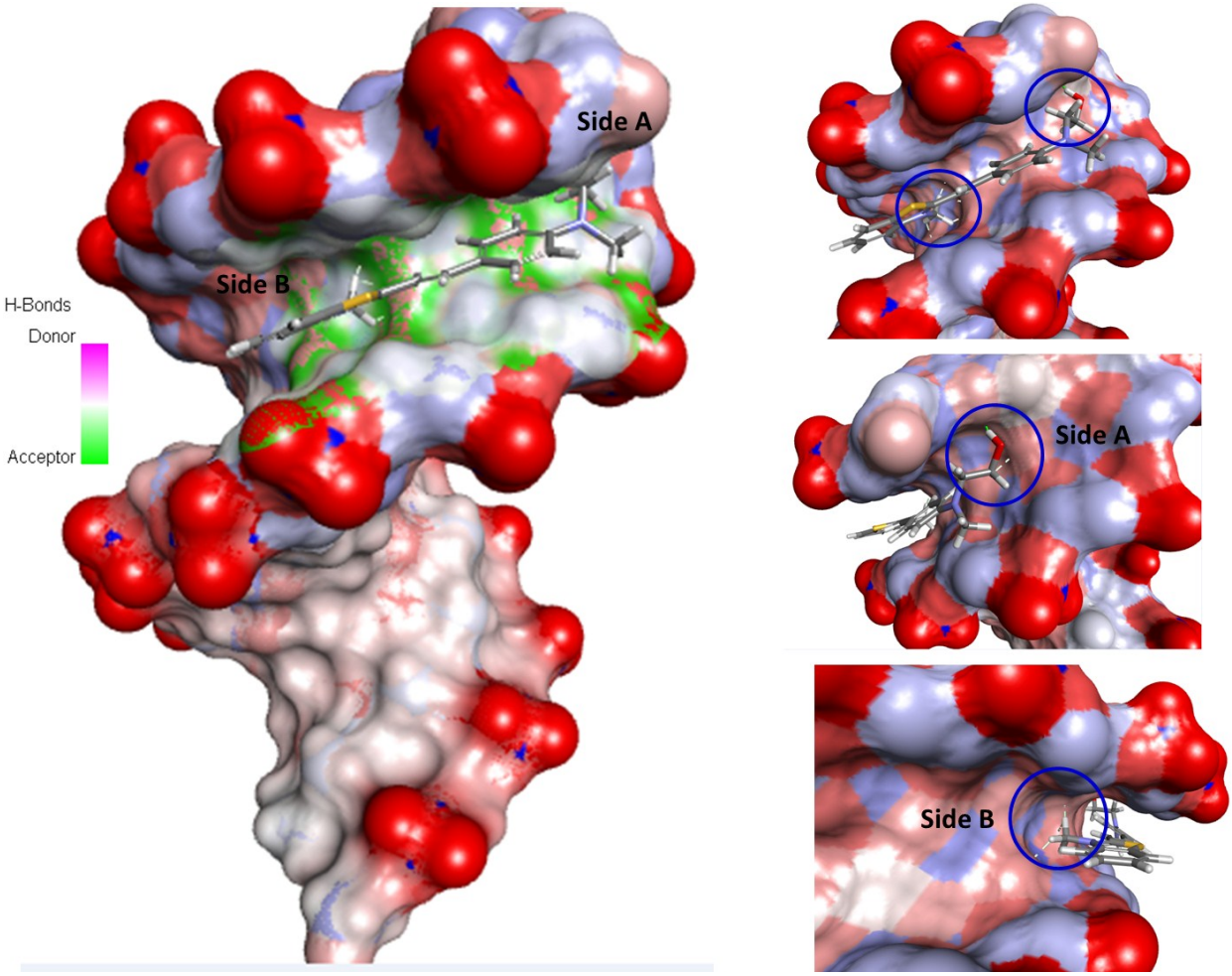

Figure S15. The side view of the interaction of DSF with DNA fragment.

(1) R. C. Weast, *CRC Handbook of Chemistry and Physics*, CRC Press Inc., Boca Raton, FL, USA, 68th ed., 1987, D221-D269.

(2) Y. Xia, Q. C. Chen, X. Y. Qin, D. D. Sun, J. N. Zhang and J. Liu, *New. J. Chem.,* 2013, **37**, 3706-3715.

(3) a) G. Cohen and H. H. Eisenberg, *Biopolymers,* 1969, **8**, 45-55; b) S. Satyanarayana, J. C. Dabrowiak and J. B. Chaires, *Biochemistry,* 1993, **32**, 2573-2584.

Characterization

^{1}H-NMR spectra of **1a**

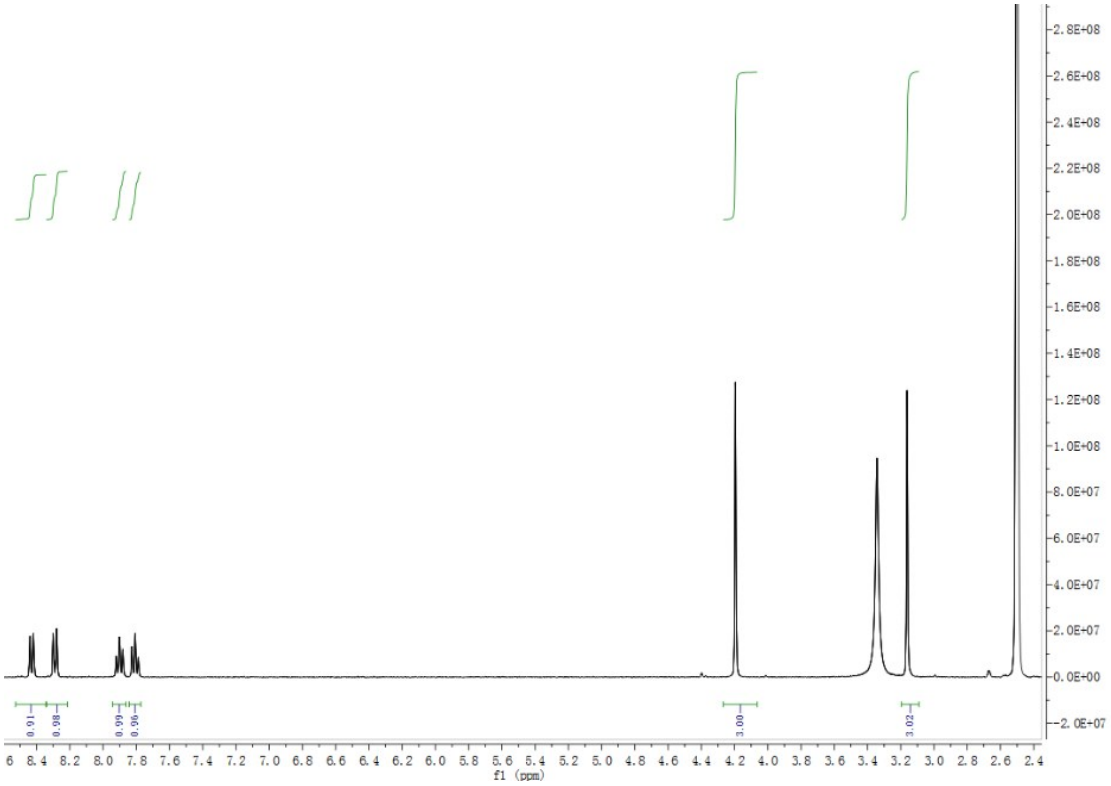

^{1}H-NMR spectra of **1b**

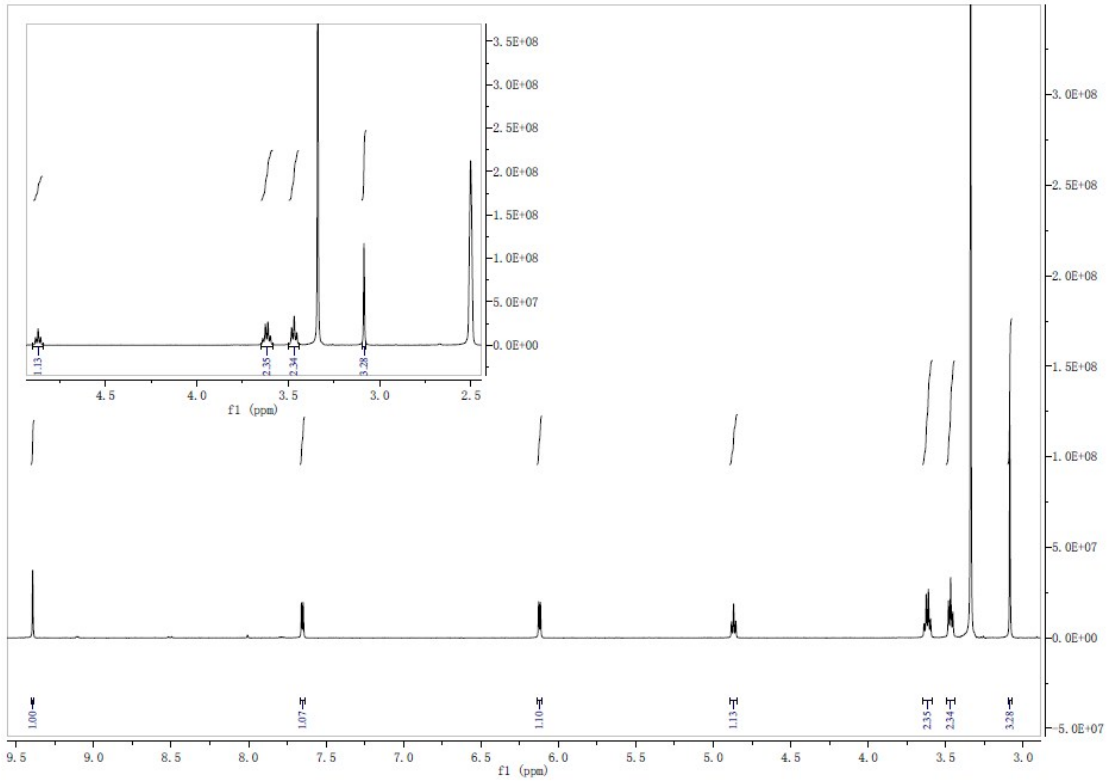

^{1}H-NMR spectra of **DSF**

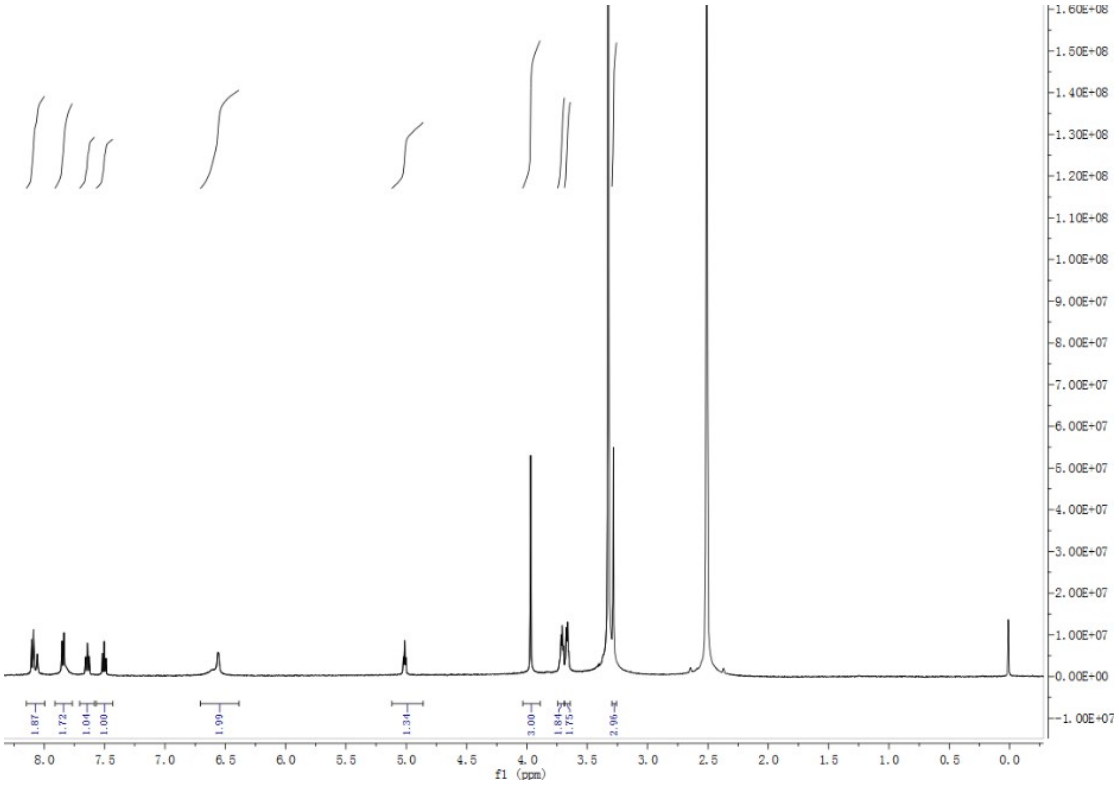

^{1}H-NMR spectra of **DBF**

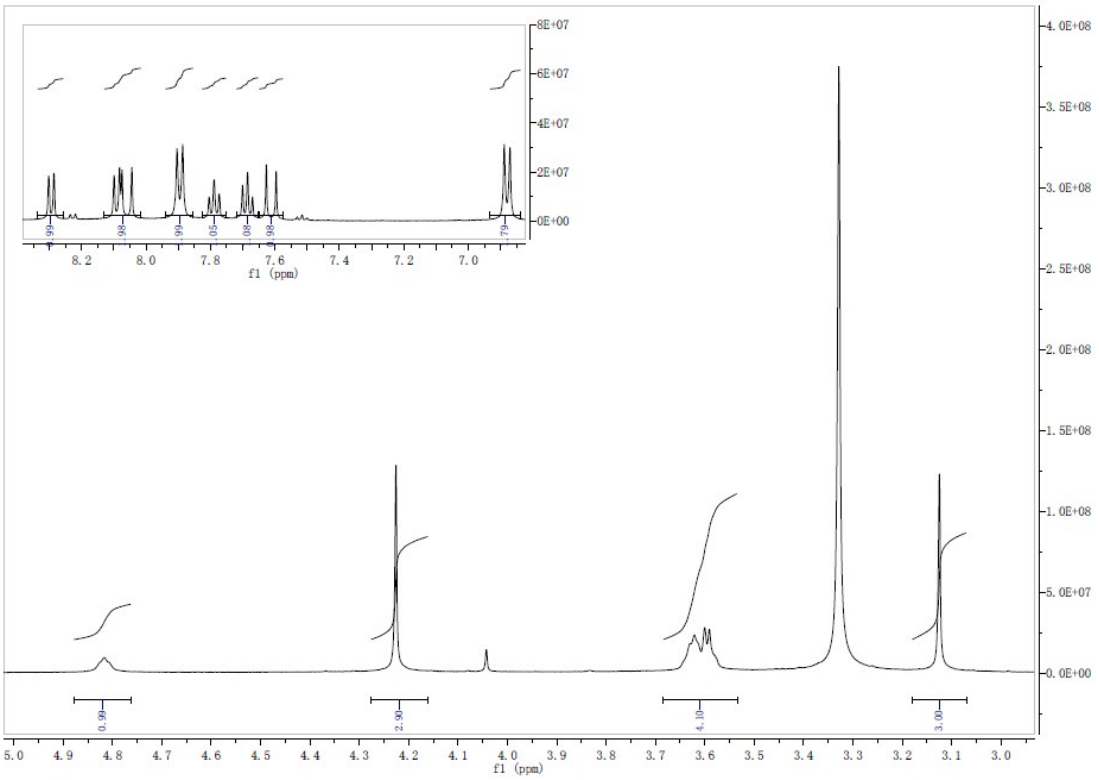

MS/ESI spectra of **DSF**

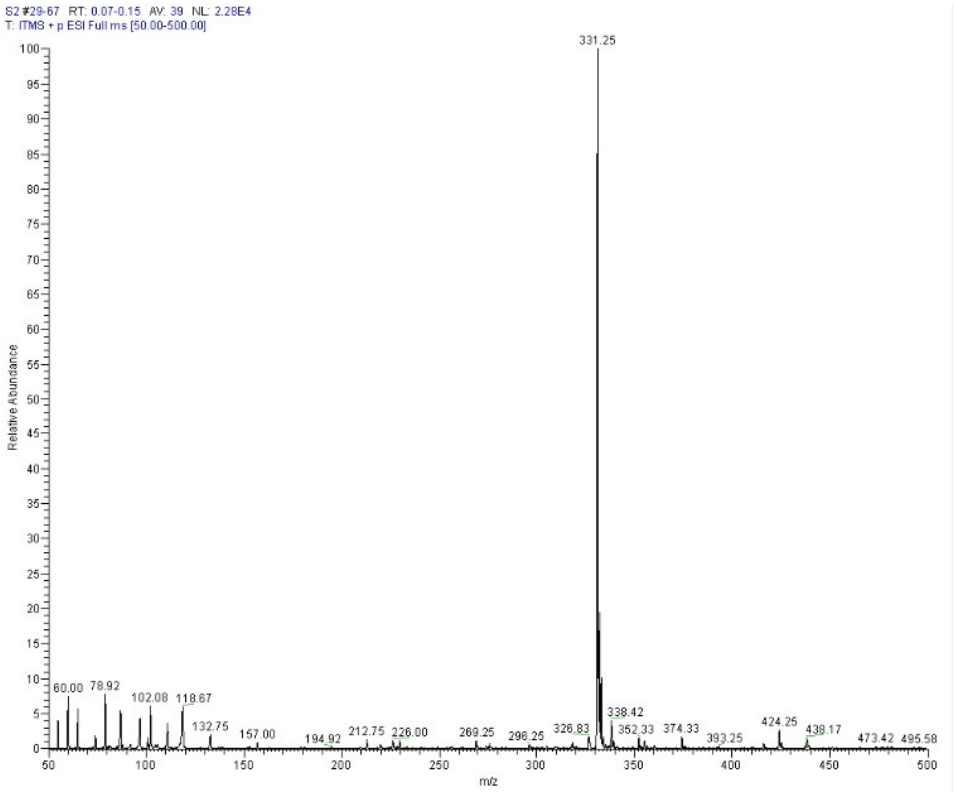

MS/ESI spectra of **DBF**

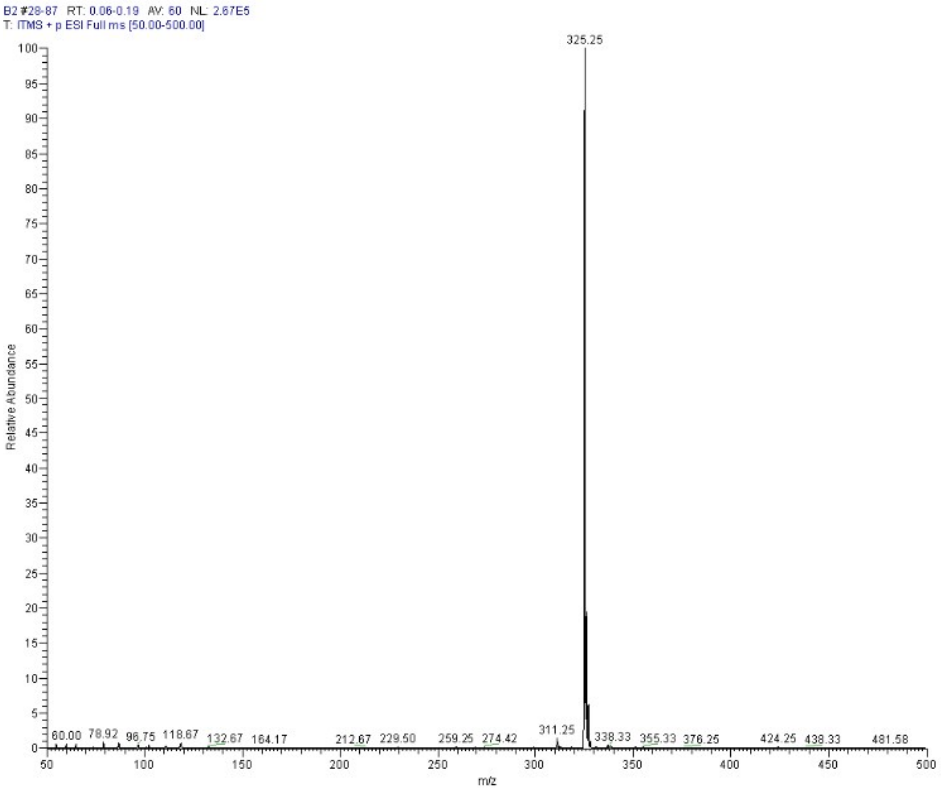
B2 #28-87 RT: 0.06-0.19 AV: 60 NL: 2.67E5
T: ITMS + p ESI Full ms [50.00-500.00]
325.25
Relative Abundance
m/z
60.00
78.92
96.75
118.67
132.67
164.17
212.67
229.50
259.25
274.42
311.25
338.33
355.33
376.25
424.25
438.33
481.58